Change of crystallization process attributes in a vacuum pan of automation systems

Viktor Sidletskyi, Oleksandr Kukhar

National University of Food Technologies, Kyiv, Ukraine

Keywords:

Sugar
Crystallization
Vacuum pan
Automation

Article history:

Received 10.11.2023
Received in revised form 27.05.2024
Accepted 2.07.2024

Corresponding author:

Viktor Sidletskyi
E-mail: vmsidletskiy@gmail.com

DOI: 10.24263/2304-974X-2024-13-2-12

Abstract

Introduction. The process of sugar crystallization is complex and non-linear, necessitating automatic control and management. However, the lack of instruments for directly measuring solution supersaturation and crystal growth highlights the need for improvements in the control system.

Materials and methods. The automation system for the process of sugar crystallization in a vacuum apparatus consists of sensors, converters of actuators, regulatory bodies, a microprocessor controller and an operator station with a SCADA program. The automation system algorithms are implemented in software in the controller and operator station.

Results and Discussion. The amount of initial syrup in the vacuum apparatus significantly affects the dry substance content in the massecuite. A high dry substance content ensures high-quality massecuite and promotes efficient crystallization. The optimal initial syrup concentration for achieving the standard dry matter content in massecuite 92% is 33%, but it can vary between 25% and 35%. An increase in the initial syrup concentration raises the average temperature of the massecuite during crystallization, which can negatively impact the final product quality. Therefore, temperature control by adjusting the initial syrup amount is crucial for optimal crystallization and producing a high-quality product.

The deformation gradient, constructed based on dry substance content and temperature parameters, reflects changes in the crystallization process. These parameters directly influence system properties, which is vital for optimizing the vacuum apparatus process. The obtained surfaces with first-rank strain tensors at 25% and 35% initial syrup values indicate changes in the strain gradient during crystallization. Key aspects such as volume change, strain tensor divergence, velocity, and acceleration are essential for calculating and analyzing the gain, time constant, and delay time in the vacuum sugar crystallization process.

Conclusions. Attributes of the crystallization process such as the amplification factor, time constant, and delay time are crucial for configuring and enhancing automated system operations, as precise calculations allow for improving control in automation systems.

Introduction

The peculiarity of the crystallization process lies in maintaining the necessary level of supersaturation of the solution, which ensures the formation and growth of crystals (Barrett et al., 2010). The supersaturation of the solution along the crystallizer determines its efficiency and requires a detailed mathematical model for control (Mazaeda et al., 2012). Due to the complexity of the process and the lack of reliable devices for direct measurement (Hassani et al., 2001), understanding the kinetics of crystal nucleation and growth, including physical mechanisms like aggregation, is crucial (Eggleston et al., 2011). Consequently, sugar crystallization is a non-linear and unstable process where key parameters such as mother liquor purity and supersaturation cannot be measured by existing sensors (Meng et al., 2019).

Studies have shown that impurities in the solution and massecuite suppress the crystallization process by specific mechanisms of inclusion on different faces of the growing crystal. These mechanisms include adsorption on the crystal surface, inclusion of liquid impurities, and co-crystallization (Azevedo et al., 1989, Schlumbach et al., 2017). A characteristic feature of the crystallization process in a vacuum apparatus is the interaction between continuous and periodic processes (Cutz et al., 2014). The main feature is that sugar crystallization is carried out in a mode that requires precise control of temperature, pressure, and steam flow, with constant adjustment in the control system (Garcia et al., 2002; Ibis, 2024; Zhang et al., 2020). This process involves cyclic heating and cooling, which affects the efficiency of evaporation (Castro et al., 2022).

Due to the lack of a reliable model describing the crystallization process, automatic crystallization control is often based on indirect measurements (Grondin-Perez et al., 2006; Lauret et al., 2000). Key parameters such as solution purity, supersaturation, crystal size, and content are difficult to measure directly (Suárez et al., 2011). The primary task of management is to monitor the supersaturation of the solution, which can be calculated through indirect measurements (Morales et al., 2023). The control process requires the use of indirect methods and mathematical models to estimate the saturation of the solution and adjust the control system settings (Bonnecaze et al., 2004; Mkwananzi et al., 2019; Prada et al., 2015).

The complexity of the crystallization process model and the adjustment of model parameters limit the possibility of its implementation in control systems (Meng et al., 2019; Villani et al., 2004). Control of the crystallization process in a vacuum apparatus has unique features due to its dynamic nature (Alvarado et al., 2024; Simoglou et al., 2005; Suárez et al., 2011). An important aspect is the effect of changing the operating mode on the transfer coefficient and the time constant of each control loop, which determine the system's response speed (Merino et al., 2018). The non-linearity of the processes means that changes in input parameters do not lead to proportional changes in output parameters, complicating the control system's operation (Zamarreño et al., 2000). The system must adapt to different phases of crystallization, fluctuations in external conditions, and wear of system components to maintain stable conditions and ensure high-quality final products (Georgieva et al., 2003; Ohara et al., 2012). This requires operators to constantly monitor and adjust settings, making the process of automating crystallization complex but necessary to achieve optimal results.

To control and analyze the quality of the crystallization process, pH measurement, dynamic light scattering, mechanical spectroscopy, and image processing methods using neural networks for automated monitoring are used (Grondin-Perez et al., 2005; Lauret et al., 2000; Meng et al., 2019). Traditional image processing methods analyze features such as shape, color, and texture but often have poor pattern generalization capabilities. In sugar crystallization, neural networks enable the creation of high-precision models for the classification of crystal images, optimizing production processes in the food industry (Grondin-Perez et al., 2005; Lauret et al., 2000; Meng et al., 2019). Accordingly, the automated system should be flexible enough to quickly respond to changes and provide effective regulation and optimal crystallization conditions (Merino et al., 2018). Furthermore, an intuitive graphical interface is essential for allowing operators to easily interact with the system (Cutz et al., 2014; Georgieva et al., 2003; Suárez et al., 2011).

Considering the measurable and non-measurable parameters of technological processes, the hierarchical and distributed nature of production inherent in food industry processes (Santos et al., 2008; Sidletskyi et al., 2019), and the specific process of sugar crystallization in a vacuum apparatus remain unresolved challenges. To address the challenges of processing large volumes of information, particularly for neural networks and artificial intelligence methods, data is presented in tensor form (Che et al., 2017; Karagoz et al., 2020). Tensor and finite element methods are already employed in electrodynamics, mechanics, gravitational field theory, elementary particle physics, the study of crystal properties, and differential geometry (Döhler et al., 2012; Hu et al., 2015). These methods were similarly used in developing a reliable regulator for aircraft (Kuntanapreeda, 2018). However, in that work, the construction of the regulator involved processing an already developed classical model in the state space using tensor analysis methods.

Given that the crystallization process is non-linear and non-stationary, and is part of the hierarchical and distributed sugar production chain, this work proposes investigating changes in the attributes of the crystallization process that affect the automation system settings. These attributes are derived from continuity equations and are presented in tensor form.

Materials and methods

The process of sugar crystallization was studied to enhance quality and reduce costs. Technical means are employed to control temperature and other parameters, followed by data analysis. Based on this analysis, trends in process parameter changes were calculated, enabling adjustments to automated control systems.

The research focuses on the crystallization of sugar in a vacuum apparatus, specifically the methods and approaches for controlling automated systems. The objective is to identify trends in the parameters of the crystallization process that influence the settings of automated control systems.

Equipment and technical means of the automation system

The automation system of the vacuum apparatus employs various technical means (Wilson et al., 1991), including sensors, converters, actuators, control bodies, a microprocessor controller (PLC – Programmable Logic Controller), and an operator station (AW) with SCADA (Supervisory Control and Data Acquisition) software (Behary et al., 2004). A fragment of the automation system, specifically the temperature and viscosity control circuits, is illustrated in Figure 1.

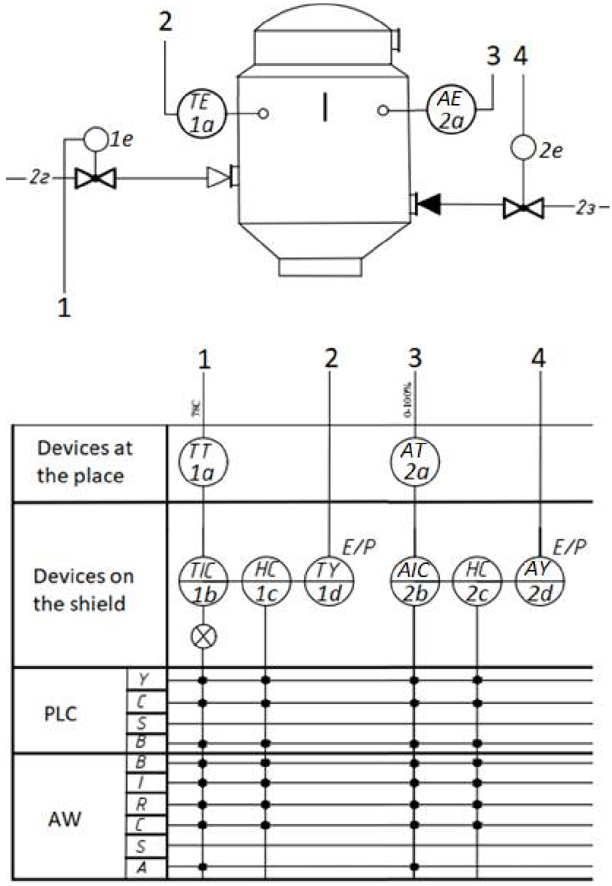

Figure 1. Fragment of vacuum apparatus automation system

TE- Temperature Element, TT – Temperature Transmitter, TIC – Temperature Indicator Controller, HC – Hand Controller, TY – Electropneumatic Converter, AE- Analytical Element, AT – Analytical Transmitter, AIC – Analytical Indicator Controller, AY – Electropneumatic Converter.

Temperature is measured using a resistance thermocouple (1a). The primary converter in device (1a), along with the converter (1a) at the site, converts the temperature value into a standardized direct current signal of 4-20 mA. The nominal supply voltage (direct current) is 24V. Since the normalizing converter is directly mounted in the measuring head of the sensor, two conductors are used to connect the converter. The standardized current signal, according to the "current loop" scheme, is sent from the normalizing converter to the secondary indicating and regulating device – the microprocessor PID regulator (1b) and to channel 4 of the controller's analog input module. The local regulator operates in manual mode when the system is started.

The control action from the analog output of the regulator, through the normally closed relay contact, or from the analog output module of the controller, through the normally open contact, is sent to the manual control unit (1c). The manual control unit is used to switch control circuits of executive devices. In automatic mode, the control action goes directly to the actuator from an external analog regulator (if manual control is necessary) or the controller. In manual mode, the control action on the actuator is formed using the built-in potentiometer (1c). The control signal from the output (1c) is sent to the electro-pneumatic converter (1d), which converts the continuous electrical DC (Direct Current) signal in the range of 4-20mA into the corresponding output analog pneumatic signal (20-100kPa). The analog pneumatic signal is fed to the integral pneumatic positioner, which is used with the pneumatic 2-way control valve (1e) to provide an accurate valve stem position proportional to the input signal received from the control device. Information about the regulator's operation is stored in the PC memory.

The high-frequency concentration analyzer is a sensor used to measure the solids in solution and massecuite (2a). The unified current signal, following the "current loop" scheme, is supplied from the normalizing converter (2a) to the secondary indicating and regulating device (11b) and to the input of the analog input module of the PLC. The control action from the analog output of the regulator is sent to the manual control unit 2b), and then to the electro-pneumatic converter (2d), which converts a continuous electrical DC in the range from 4 to 20 mA into a corresponding output analog pneumatic signal (20 – 100 kPa). This pneumatic signal is supplied to an integral pneumatic positioner, which is used with the SAMSON 3278 (2e) pneumatic 2-way control valve to ensure precise valve stem positioning proportional to the input signal from the control device.

Processing of incoming information

Data on the operation of the crystallization process and the control system are stored in the operator station (AW) with the SCADA program. The stored data consists of a set of time-stamped parameter values (Dogbe et al., 2018).

Based on the saved data, attributes (amplification factor, time constant, delay time) of the crystallization process necessary for calculating the settings of the vacuum apparatus automation system are determined. To evaluate changes in gain, time constant, and delay time, factors such as strain gradient, volume, divergence, velocity, and acceleration are considered.

Results and discussion

Representation of the technological process of crystallization in tensor form

The importance of the initial syrup amount in the vacuum apparatus is determined by its effect on the dry substance content in massecuite. Studies have shown that to achieve the normative dry substance content in massecuite ($CP_{massecuite}$ = 92%) the optimal initial syrup value is $G_{beginning}$ = 33% (Kotcubansky et al., 2012). High dry substance content ensures high-quality massecuite and contributes to an efficient crystallization process. Thus, controlling the initial syrup amount is crucial to obtaining a product of the required quality and avoiding issues associated with excessive massecuite viscosity, which can negatively impact crystallization. The initial syrup amount also significantly affects the dry substance content in the intercrystalline solution. An increase in the dry substance content in the solution worsens crystallization conditions due to higher sugar solution viscosity, which complicates heat transfer and raises the solution's average temperature (Kotcubansky et al., 2012). This leads to increased sucrose solubility and thermal decomposition, adversely affecting the final product. Therefore, maintaining the optimal initial syrup amount is critical for the stability and efficiency of the crystallization process.

Temperature also varies significantly with the initial syrup amount. A higher initial syrup concentration leads to an increased average massecuite temperature during crystallization, which can negatively affect the final product quality (Kotcubansky et al., 2012). Elevated temperatures contribute to sucrose decomposition, reducing crystalline sugar yield and quality. Thus, temperature control by adjusting the initial syrup amount is vital for ensuring an optimal crystallization process and achieving a high-quality product.

Considering the above, the values $[C_{ut}, C_r, T]$, were formed based on the dry substance content in the solution and massecuite, accounting for temperature regimes for different initial syrup values, where (C_{ut}) – is the dry substance content in massecuite, (C_r) – is the dry substance content in the solution, and (T) – is the temperature. The vector $X_i = [x_{1i}, x_{2i}, x_{3i}]^T$ represents the initial syrup value, and vector $Y_i = [y_{1i}, y_{2i}, y_{3i}]^T$ represents the changed technological mode. Vector multiplication results in a surface in local spatial coordinates (Sidletskyi, 2019). Figure 2 illustrates the transition to spatial local coordinates.

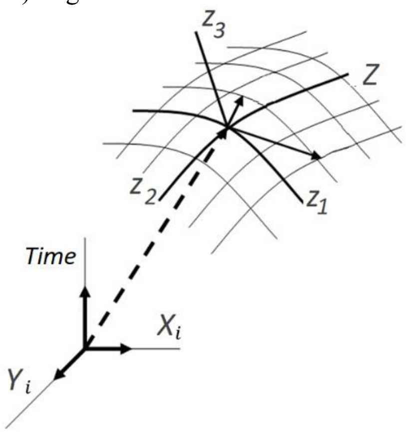

Figure 2. Transition from one technological regime to another depicted in local spatial coordinates

The deformation tensor is defined as the derivative of the displacement vector along spatial coordinates, describing how material points move relative to each other in space (Sperling et al., 2023). The strain gradient $\boldsymbol{F}$ describes changes in the position of a material point in space, encompassing linear transformations such as rotation and stretching, and is a rank 2 tensor (Baár et al., 2020; Horák et al., 2019, Sidletskyi et al., 2020):

$$F = \begin{pmatrix} \frac{\partial x}{\partial X} & \frac{\partial x}{\partial Y} & \frac{\partial x}{\partial Z} \\ \frac{\partial y}{\partial X} & \frac{\partial y}{\partial Y} & \frac{\partial y}{\partial Z} \\ \frac{\partial z}{\partial X} & \frac{\partial z}{\partial Y} & \frac{\partial z}{\partial Z} \end{pmatrix} \tag{1}$$

where x, y, z are the current coordinates of the point, and X, Y, Z are the initial coordinates.

The deformation tensor E is a symmetric tensor of the 2nd rank, describing quadratic deformations without considering rotation. It is related to internal deformations and the deformation energy of the material, defined through the deformation gradient F:

$$\mathbf{E} = \frac{1}{2}(\mathbf{F^T F} - \mathbf{I}) \tag{2}$$

where I is the identity matrix.

For a general description of the energy balance (Loubser, 2004; Petrenko et al., 2020; Singh, 2019) of the thermal crystallization process, the thermal conductivity equations were used:

$$\rho c_p \left(\frac{\partial T}{\partial t} + \boldsymbol{v} \cdot \nabla T\right) = \nabla \cdot (k \nabla T) + Q \tag{3}$$

where:
- T is temperature, (K)
- c_p is specific heat capacity, (J/(kg·K))
- k is thermal conductivity, (W/(m·K))
- Q represents heat sources, (W)
- ρ is the density (concentration of dry substances), (kg/m³)
- ∇ denotes divergence (vector operator)
- $\boldsymbol{v}$ is the velocity of the material (m/s)

To describe the mass balance (Hassani et al., 2001; Hrama et al., 2019; Pohorilyi, 2023; Suárez et al., 2011), which accounts for the change in dry substance concentration in the massecuite and solution, the equation is:

$$\frac{\partial \rho}{\partial t} + \nabla \cdot (\rho v) = 0 \tag{4}$$

where:
- ρ is the density (concentration of dry substances),
- $\boldsymbol{v}$ is the velocity of the material.

By combining these equations, we get:

For mass balance:

$$\frac{\partial \rho}{\partial t} + \nabla \cdot (\rho v) + \rho(\nabla \cdot F) = 0 \tag{5}$$

For heat balance:

$$\rho c_p \left(\frac{\partial T}{\partial t} + \boldsymbol{v} \cdot \nabla T\right) = \nabla \cdot (k \nabla T) + Q + \rho c_p (\nabla \cdot F) T \tag{6}$$

For concentration change:

$$\frac{\partial C}{\partial t} + \nabla \cdot (C \boldsymbol{v}) = D \nabla^2 C + C(\nabla \cdot F) \tag{7}$$

where:
- C is the concentration of dry substances, (kg/m³),
- D is the diffusion coefficient (m²/s).

The additional terms $\rho(\nabla \cdot F)$ і $\rho c_p (\nabla \cdot F) T$ в account for volume change due to the strain gradient.

The divergence of the deformation tensor $\nabla \cdot F$ characterizes the volume change in the system (Wang et al., 2020). Divergence of the deformation gradient:

$$\nabla \cdot F = \frac{\partial F}{\partial X} + \frac{\partial F_{22}}{\partial Y} + \frac{\partial F_{33}}{\partial Z} \tag{8}$$

Considering the deformation gradient and its divergence in the continuity equations for mass and heat allows for the accurate description of mass and energy transfer processes in the crystallization system, including volume change, dry substance concentration, and temperature distribution. Therefore, the divergence of the deformation gradient $\nabla \cdot \boldsymbol{F}$ can be considered an indicator of changes in the internal state of the system, which can be used as an amplification factor in the automated control system.

Control system parameters as components of the deformation gradient of the technological process

In our case, the divergence of the deformation gradient shows how quickly the system parameters (solids content and temperature) change in space. This can be interpreted as a measure of the sensitivity or gain that the system applies to its internal parameters (Chowdhury et al., 2022; Pedersen et al., 2015; Tabassum et al., 2024; Tuttle et al., 2021). If the divergence of the strain gradient is large, it may indicate high concentration and temperature gradients, suggesting rapid changes in the system. Thus:

$$K_p = \nabla \cdot F \tag{9}$$

where K_p is the amplification factor determined by the divergence of the deformation gradient.

The speed and acceleration of the deformation gradient can be interpreted as dynamic characteristics of the system. Accordingly, the time constant τ is a characteristic of a dynamic system that determines how quickly the system responds to changes in the input signal. In first-order systems, this is the time it takes for the system response to reach approximately 63% of its final value after a disturbance. The delay time T_d is the time delay between the application of a disturbance to the system and the start of its response.

To determine the time constant and delay time of the system, consider a simplified model of a first-order system with a delay:

$$G(s) = \frac{Ke^{-T_d s}}{\tau s + 1} \tag{10}$$

where $G(s)$ is the transfer function of the system, K is the gain factor, τ is the time constant, and T_d is the delay time.

The rate of change of parameters (such as the concentration of dry substances or temperature) can be linked to the time constant of the system. A high rate indicates a fast response to changes, suggesting a smaller time constant.

Acceleration, representing the change in velocity over time, is related to the dynamic response characteristics of the system. However, additional aspects must be considered to determine the delay time accurately.

As previously mentioned, it is assumed that the deformation gradient F describes the change in the concentration of dry substances and temperature. Thus, the rate of change of the deformation gradient can be expressed as:

$$v = \frac{\partial F}{\partial t} \tag{11}$$

Acceleration characterizes the change in speed over time, aiding in the evaluation of the system's dynamic behavior and potential delays:

$$a = \frac{\partial^2 F}{\partial t^2} \tag{12}$$

The time constant τ can be estimated as the inverse of the system response rate:

$$\tau \approx \frac{1}{|v|} \tag{13}$$

An analysis of the system's response to a disturbance can estimate the delay time. If there is a known delay before the system begins to change parameters, this delay time can be estimated as:

$$T_d \approx \frac{1}{|a|} \tag{14}$$

Deformation gradient in local spatial coordinates

When studying the crystallization process in the vacuum apparatus, 25% initial loading and 35% final loading were used. According to (Kotcubansky et al., 2012), this approach allows for a comprehensive understanding of the crystallization process at different loading levels. This choice enables the analysis of a wide range of syrup concentrations, which helps to investigate how concentration changes affect the crystallization process. Analyzing the range of possible changes in the technological process is necessary to obtain optimal process conditions. The resulting parameter changes, from the initial to the final stage, reflect the dynamics of the process. This approach facilitates understanding how heat is effectively transferred at different syrup concentrations, which is crucial for maintaining a stable crystallization process and avoiding overheating or underheating (Kotcubansky et al., 2012, Petrenko et al., 2020, Pohorilyi, 2023). This comprehensive analysis of the crystallization process allows for the optimization of technological parameters and ensures high quality of the final product. Figures 3 and 4 present simplified graphs of the content of dry substances in massecuite, the content of dry substances in the solution, and temperature. The graphs were constructed by interpolating the points given in (Kotcubansky et al., 2012).

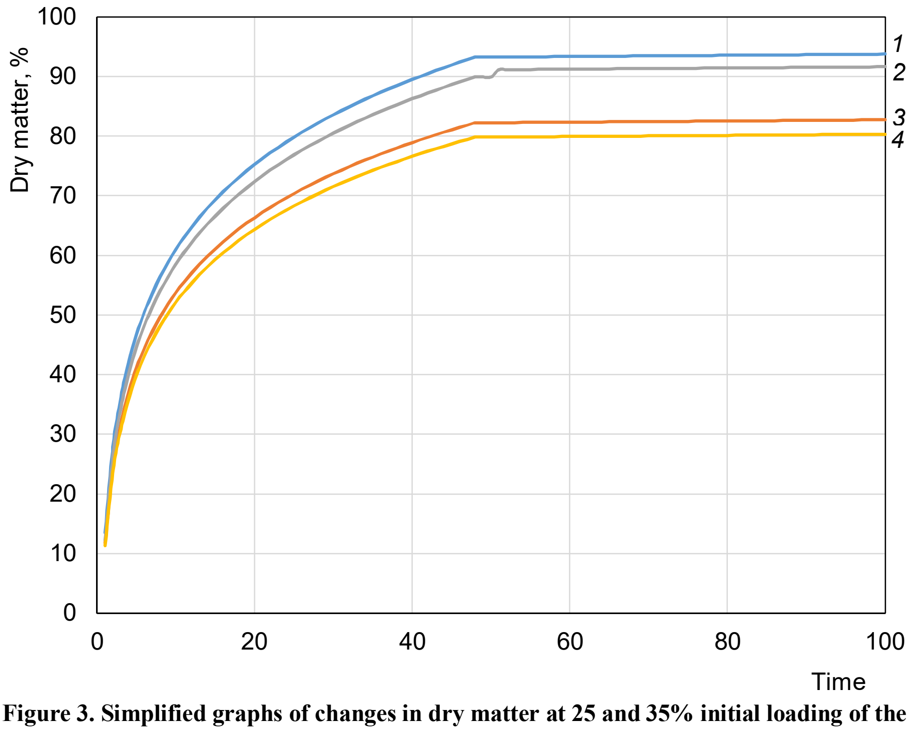

Figure 3. Simplified graphs of changes in dry matter at 25 and 35% initial loading of the apparatus:
1 – Dry matter in massecuite for 25% from initial loading of the apparatus;
2 – Dry matter in syrup for 25% from initial loading of the apparatus;
3 – Dry matter in massecuite for 35% from initial loading of the apparatus;
4 – Dry matter in syrup for 35% from initial loading of the apparatus;
*Time – dimensionless time, calculated as the ratio of the current time to the total crystallization time.

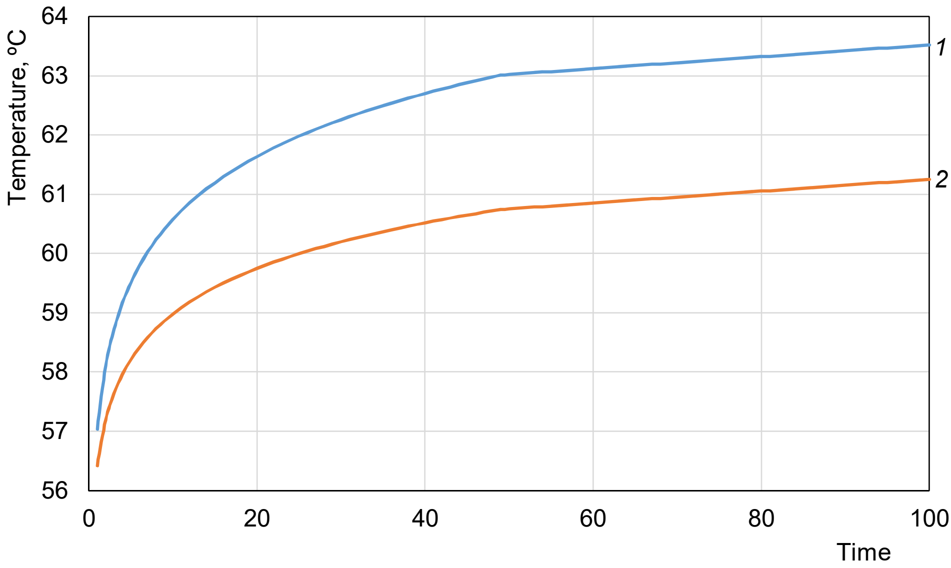

Figure 4. Simplified graphs of temperature changes at 25% and 35% from initial loading of the apparatus:
1 – Temperature mode for 25% from initial loading of the apparatus;
2 – Temperature mode for 35% from initial loading of the apparatus.
*Time – dimensionless time, calculated as the ratio of the current time to the total crystallization time.

Based on the data shown in Figures 3 and 4, and the dependencies in Section 2.3, the surfaces of the deformation gradient of the crystallization process in spatial coordinates were obtained. For analysis, the data were modified as follows:

– Figure 5a: The surface is constructed at 25% and 35% from initial loading of the device using the data shown in Figures 3 and 4.
– Figure 5b: The surface is constructed at 25% and 35% from initial loading of the device, but for the 25% mode, the temperature is considered constant with the initial value.
– Figure 5c: The surface is constructed at 25% and 35% from initial loading of the device, but for the 35% mode, the temperature is considered constant with the initial value.
– Figure 5d: The surface is constructed at 25% and 35% from initial loading of the apparatus, with temperatures considered constant with the initial value.

After analyzing the obtained surfaces, we found that surfaces a and d have the most significant changes. Therefore, for further calculations and research, the corresponding deformation gradients of the crystallization process were taken. The deformation gradient constructed according to the parameters of dry substance content and temperature reflects changes in the crystallization process. These parameters directly affect the system properties, which is crucial for optimizing the process in a vacuum apparatus.

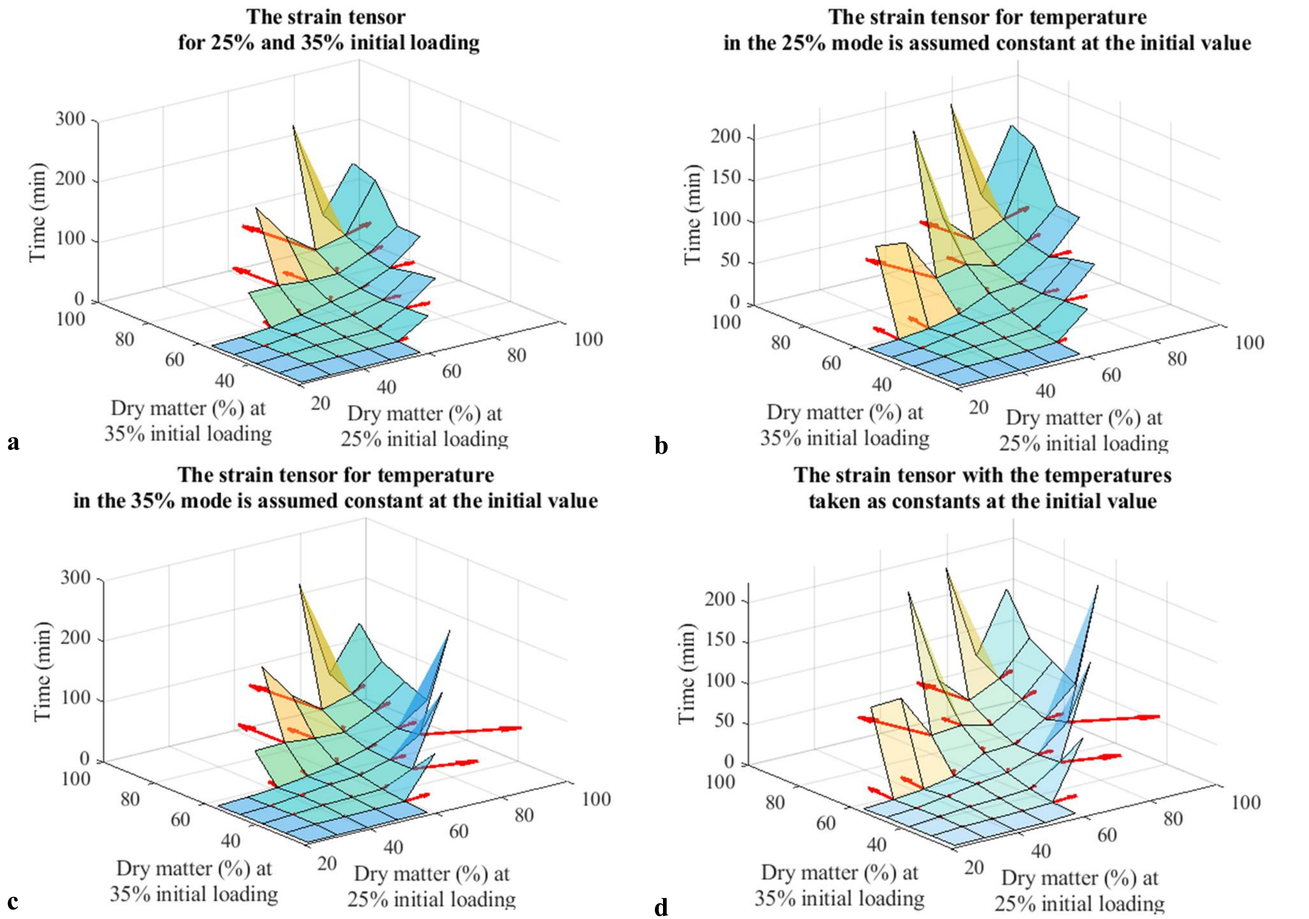

Figure 5. The strain tensors constructed at 25% and 35% from initial loading of the device and the data shown in Figures 3 and 4

Amplification factor for the vacuum apparatus at different loading values

Figures 6 and 7 show the changes in the volume of the deformation gradient and the divergence of the deformation tensor at 25% and 35% from initial loading of the apparatus. These are key aspects for calculating and analyzing the amplification factor in the crystallization process of sugar in a vacuum apparatus.

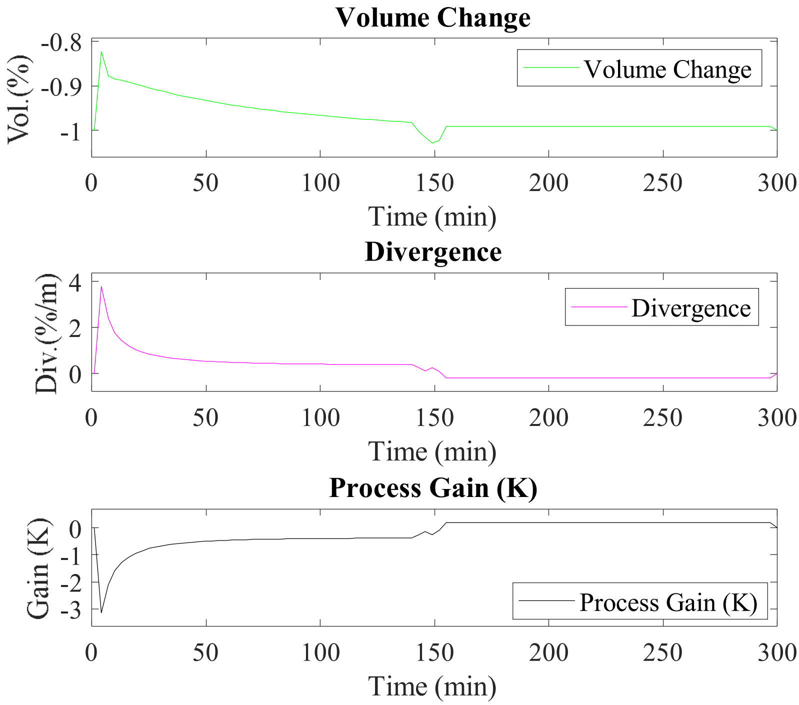

Figure 6. Volume, divergence, and amplification factor at 25% and 35% from initial loading of the device and the data shown in Figures 3 and 4.

The change in the volume of the deformation gradient reflects the interaction between the thermal and mechanical properties of sugar during crystallization. Considering these changes allows for accurate modeling of heat transfer and mechanical stresses affecting the crystallization rate. The divergence of the deformation gradient, which shows the spatial distribution of deformations, helps identify areas with the highest concentration of mechanical influences. This provides a more detailed process analysis, enabling the determination of optimal conditions for achieving the desired gain.

By analyzing changes in the volume and divergence of the deformation gradient, it is possible to accurately determine the parameters affecting the efficiency of the crystallization process. For example, changes in the volume of the deformation gradient help assess the influence of pressure and temperature on sugar crystal formation. Divergence shows how changes in mechanical stress affect the uniformity and size of crystals. This allows for the optimization of conditions in the vacuum apparatus to achieve the maximum amplification factor, critical for industrial process efficiency. Consequently, using these parameters provides a deeper understanding of the crystallization mechanisms, improving the quality of the final product

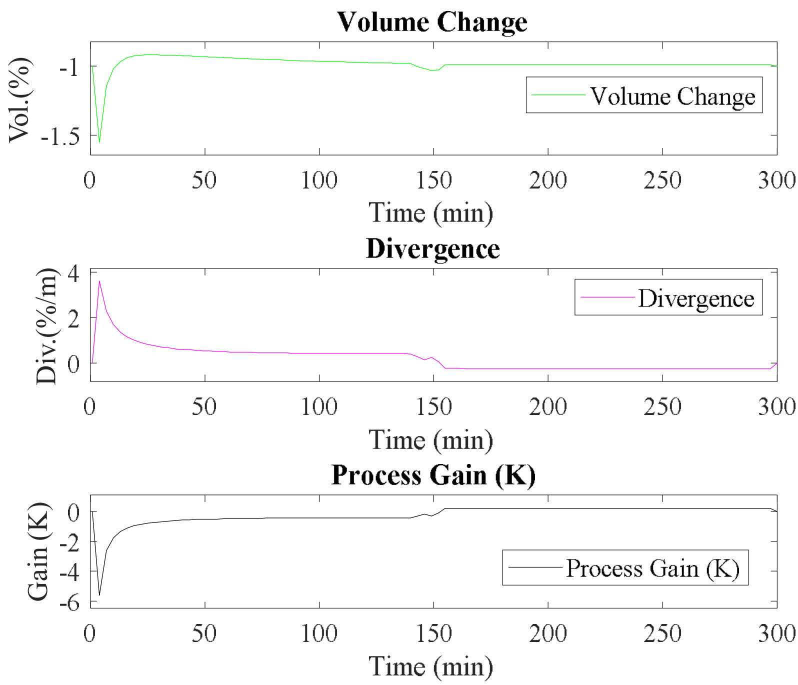

Figure 7. Volume, divergence, and amplification factor at 25% and 35% from initial loading of the device and the data shown in Figures 3 and 4 with constant process temperatures.

Changes in speed and acceleration as components of the constant time and delay time for the vacuum apparatus at different loading values

The change in the volume of the deformation gradient and the divergence of the deformation gradient allow for the calculation and analysis of the rate of change in velocity and acceleration during the sugar crystallization process in a vacuum apparatus. By analyzing these parameters, we can determine how quickly crystallization conditions respond to changes in thermal and mechanical conditions. This, in turn, allows us to calculate the time constant, which characterizes the speed of the process's reaction to changing conditions. Measuring acceleration, as the second derivative of the deformation gradient, helps assess the system's dynamic properties and identify potential instabilities. These parameters thus assist in precisely regulating the process to achieve optimal crystallization conditions.

Furthermore, the divergence of the deformation gradient helps determine the delay time, which is crucial for controlling the crystallization process. Divergence indicates moments when changes in one part of the system affect other parts, which is essential for accurately predicting the system's behavior. Considering the delay time helps adjust the control system to compensate for these delays and ensure stable operation of the vacuum apparatus. Overall, analyzing changes in velocity and acceleration based on the deformation gradient provides a deeper understanding of the dynamic characteristics of the process. This allows for the optimization of control parameters and improves the efficiency of sugar crystallization.

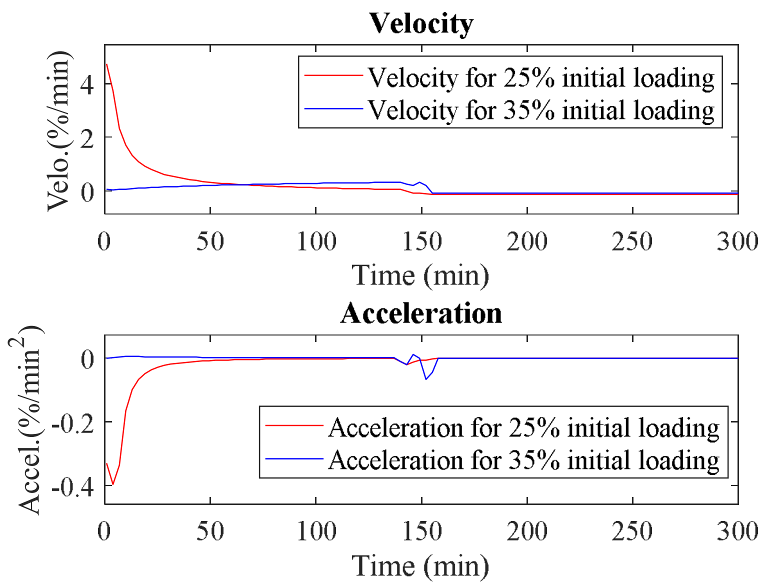

Figure 8. Speed and acceleration as components of the time constant and delay time for the deformation gradient at 25% and 35% from initial loading of the apparatus, based on data presented in Figures 3 and 4.

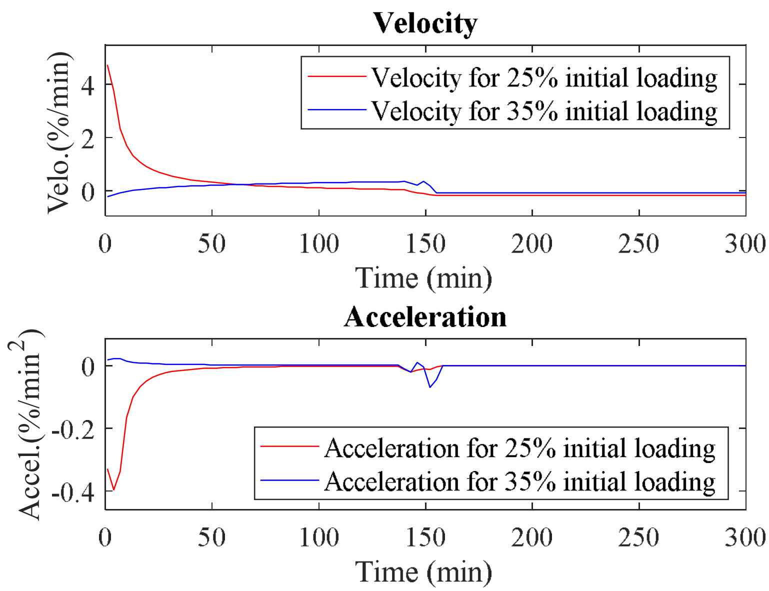

Figure 9. Speed and acceleration for 25% and 35%from initial loading of the apparatus, based on data presented in Figures 3 and 4 and constant process temperature values.

Thus, the velocity and acceleration of the deformation gradient can provide insights into the time constant and delay time of an object in an automated control system. The rate of change of parameters indicates the time constant, as it characterizes the system's response speed, while acceleration can highlight dynamic aspects related to delays in the system's response. However, accurately defining these characteristics requires a more detailed analysis of the system and its dynamic properties.

Using the deformation gradient and tensor, continuity equations, and balance equations allows for more precise modeling of complex physical processes. This is particularly important for the crystallization process, where it is necessary to consider thermodynamic and physicochemical features. These advantages in calculating parameters such as the time constant, amplification factor, and delay time provide better regulator settings to maintain the desired technological process in sugar crystallization. This is mainly due to accounting for temperature changes and the crystallization kinetics of dry substance content in the solution and massecuite.

However, models based on continuity equations and deformation gradients are much more complex and require more computational resources to solve. This can be problematic in real-world applications, especially for large systems. This complexity explains the use of tensor approaches for description and calculation, which allow processing significant amounts of data and information.

Conclusions

1. Strain gradients constructed on the basis of vectors including information on dry matter content and temperature can provide a complete picture of the crystallization process in a vacuum apparatus. This allows to model and control the process more accurately, providing effective management and optimization of the process.
2. The obtained values of the divergence of the deformation gradient as input parameters for the controller make it possible to evaluate and respond to changes in concentrations and temperature, regulating the processes to achieve the desired crystallization conditions. In an automated control system, such an indicator can be used to adjust control algorithms in order to stabilize the process or optimize crystallization conditions.
3. The divergence of the deformation gradient $\nabla \cdot \boldsymbol{F}$ can be used as an indicator of changes in the internal state of the system and considered as a gain factor in an automated control system. This allows taking into account the rate of change of system parameters, such as solids content and temperature, and adjusting control mechanisms accordingly for optimal control of the crystallization process.
4. Velocity and acceleration, as position-time derivative and velocity-time derivative, respectively, allow real-time process control and correction, which is critical for achieving a stable and efficient crystallization process.
5. The rate and acceleration of the deformation gradient, constructed on the basis of data on the content of solids in the massecuite, the content of solids in the solution and the temperature of the crystallization process, are information about the time constant and the delay time of the object in the automated control system.

References

Alvarado J.P., Palma H.H., Ramos C.G., Moreno-Ríos A.L., Osio E.M., Horta R.G., Caraveo G.I., Moreno S.E. (2024), Evaporation automation at the Central de Mieles de Útica, Colombia, for non-centrifugal sugar cane production: Sustainable optimization strategies, *Bioresource Technology Reports*, 26, 101850, https://doi.org/10.1016/j.biteb.2024.101850

Azevedo S.F., Gonçalves M.J., Ruiz V., Najim K. (1989), Generalized Predictive Control of a Batch Evaporative Crystallizer, *IFAC Proceedings Volumes*, 22, pp. 93–98, https://doi.org/10.1016/S1474-6670(17)53342-X

Baár T., Bauer P.H., Luspay T. (2020), Decoupling of discrete-time dynamical systems through input-output blending, *IFAC-PapersOnLine*, 53, pp. 921–926, https://doi.org/10.1016/j.ifacol.2020.12.856

Barrett M., McNamara M., Hao, H., Barrett P., Glennon B. (2010), Supersaturation tracking for the development, optimization and control of crystallization processes, *Chemical Engineering Research & Design*, 88, pp. 1108–1119, https://doi.org/10.1016/j.cherd.2010.02.010

Behary M.S., Ah King R.T., Rughooputh H.C. (2004), Automation of sugar boiling process in batch vacuum pans using ABB-Freelance PLC (AC 800F) and conductor NT SCADA, *2004 IEEE International Conference on Industrial Technology, 2004 IEEE ICIT '04*, 2, pp. 853–858, https://doi.org/10.1109/ICIT.2004.1490186

Castro R.E., Alves R.M., Nascimento, C.A. (2022), Dynamic Simulation of Multiple-Effect Evaporation, *SSRN Electronic Journal*, 34, pp. 1–14, http://dx.doi.org/10.2139/ssrn.4021873

Che M., Cichocki A., Wei Y. (2017), Neural networks for computing best rank-one approximations of tensors and its applications, *Neurocomputing*, 267, pp. 114–133, https://doi.org/10.1016/j.neucom.2017.04.058

Chowdhury M.A., Lu Q. (2022), A novel entropy-maximizing TD3-based reinforcement learning for automatic PID Tuning, *2023 American Control Conference (ACC)*, pp. 2763–2768, https://doi.org/10.23919/ACC55779.2023.10156246

Cutz L., Santana D. (2014), Techno-economic analysis of integrating sweet sorghum into sugar mills: The Central American case, *Biomass and Bioenergy*, 68, pp. 195–214, https://doi.org/10.1016/j.biombioe.2014.06.011

Dogbe E.S., Mandegari M., Görgens J.F. (2018), Exergetic diagnosis and performance analysis of a typical sugar mill based on Aspen Plus® simulation of the process, *Energy*, 145, pp. 614–625, https://doi.org/10.1016/j.energy.2017.12.134

Döhler M., Mevel L. (2012), Fast multi-order computation of system matrices in subspace-based system identification, *Control Engineering Practice*, 20, pp. 882–894, https://doi.org/10.1016/j.conengprac.2012.05.005

Eggleston G., Ĉoté G.L., Santee C.J. (2011), New insights on the hard-to-boil massecuite phenomenon in raw sugar manufacture, *Food Chemistry*, 126, pp. 21–30, https://doi.org/10.1016/j.foodchem.2010.10.038

Garcia A., Acebes L., Prada C.D. (2002), Modelling and simulation of batch processes: a case study, *IFAC Proceedings,* 35, pp. 169–174, https://doi.org/10.3182/20020721-6-ES-1901.01014

Georgieva P., Meireles M., Azevedo S.F. (2003), Knowledge-based hybrid modelling of a batch crystallisation when accounting for nucleation, growth and agglomeration phenomena, *Chemical Engineering Science*, 58, pp. 3699–3713, https://doi.org/10.1016/S0009-2509(03)00260-4

Grondin-Perez B., Benne M., Bonnecaze C., Chabriat J. (2005), Industrial multi-step forward predictor of mother liquor purity of the final stage of a cane sugar crystallisation plant,

Journal of Food Engineering, 66, 361–367, https://doi.org/10.1016/j.jfoodeng.2004.04.002
Grondin-Perez B., Benne M., Chabriat J. (2006), Supervision of C crystallisation in Bois Rouge sugar mill using on-line crystal content estimation using synchronous microwave and refractometric brix measurements, *Journal of Food Engineering*, 76, pp. 639–645, https://doi.org/10.1016/j.jfoodeng.2005.06.014
Hassani N.S., Saidi K., Bounahmidi T. (2001), Steady state modeling and simulation of an industrial sugar continuous crystallizer, *Computers & Chemical Engineering*, 25, pp. 1351–1370, https://doi.org/10.1016/S0098-1354(01)00705-0
Horák M., Kružík M. (2019), Gradient polyconvex material models and their numerical treatment, *International Journal of Solids and Structures*, 195, pp. 57–65, https://doi.org/10.1016/j.ijsolstr.2020.03.006
Hu Y., Li T., Fan C., Wang D., Li J. (2015), Three-dimensional tensor controlled-source electromagnetic modeling based on the vector finite-element method, *Applied Geophysics*, 12, pp. 35–46, https://doi.org/10.1007/s11770-014-0469-1
Ibis O.I., Bugday Y.B., Aljurf B.N., Goksu A.O., Solmaz H., Oztop M.H., Sumnu, G. (2023), Crystallization of sucrose by using microwave vacuum evaporation, *Journal of Food Engineering*, 365(10), 111847, https://doi.org/10.1016/j.jfoodeng.2023.111847
Karagoz R., Batselier K. (2020), Nonlinear system identification with regularized Tensor Network B-splines, *Automatica*, 122, 109300, https://doi.org/10.1016/j.automatica.2020.109300
Kotcubansky A.M., Mironchuk V.H., (2012), Efficient by initial syrups vacuum pan for boiling restorative sugar solution, *Ukrainian Food Journal*, 1, pp 81-85.
Kuntanapreeda S. (2018). Control of shimmy vibration in aircraft landing gears based on tensor product model transformation and twisting sliding mode algorithm, *MATEC Web of Conferences*, 161, 02001, https://doi.org/10.1051/matecconf/201816102001
Lauret A.J., Boyer H., Gatina J.C. (2000), Hybrid modelling of a sugar boiling process, *Control Engineering Practice*, 8, 299–310, https://doi.org/10.1016/S0967-0661(99)00151-3
Loubser R.C. (2004), Heat and mass balance using constraint equations, a spreadsheet, and the newton-raphson technique, *Proceedings of the 78th Annual Congress of South African Sugar Technologists' Association, held at Kwa-Shukela, Mount Edgecombe, South Africa, 27-30 July 2004,* 78, pp. 457–471.
Mazaeda R., Gómez A.M., Moraga C.D., Arconada L.F. (2012), Hybrid modelling of batch centrifuges as part of a generic object oriented beet Sugar Mill library, *Simulation Modelling Practice and Theory*, 22, pp. 123–145, https://doi.org/10.1016/j.simpat.2011.12.003
Meng Y., Yu S., Zhang J., Qin J., Dong Z., Lu G., Pang H.F. (2019), Hybrid modeling based on mechanistic and data-driven approaches for cane sugar crystallization, *Journal of Food Engineering*, 257, pp. 44–55, https://doi.org/10.1016/j.jfoodeng.2019.03.026
Merino A., Acebes L., Alves R., Prada C.D. (2018), Real Time Optimization for steam management in an evaporation section, *Control Engineering Practice*, 79, pp. 91–104, https://doi.org/10.1016/j.conengprac.2018.07.010
Mkwananzi T., Mandegari M., Görgens J.F. (2019), Disturbance modelling through steady-state value deviations: The determination of suitable energy indicators and parameters for energy consumption monitoring in a typical sugar mill, *Energy*, 176, pp. 211–223, https://doi.org/10.1016/j.energy.2019.03.191
Morales H., Sciascio F.D., Aguirre-Zapata, E., Amicarelli A.N. (2023), A model-based supersaturation estimator (inferential or soft-sensor) for industrial sugar crystallization process, *Journal of Process Control*, 129, pp. 839–844, https://doi.org/10.1016/j.jprocont.2023.103065
Ohara S., Fukushima Y., Sugimoto A., Terajima Y., Ishida T., & Sakoda, A. (2012), Rethinking the cane sugar mill by using selective fermentation of reducing sugars by *Saccharomyces*

dairenensis, prior to sugar crystallization, *Biomass and Bioenergy*, 42, pp. 78–85, https://doi.org/10.1016/j.biombioe.2012.03.024

Pedersen T., Godhavn J., Schubert J.J. (2015), Supervisory control for underbalanced drilling operations, *IFAC-PapersOnLine*, 48, pp. 120–127, https://doi.org/10.1016/j.ifacol.2015.08.019

Petrenko V., Zasyadko Y., Pryadko M. (2020), Modeling of heat transfer deterioration regimes when concentrating solutions in industrial film evaporators, *Ukrainian Food Journal*, 9(4), pp. 901-916, https://doi.org/10.24263/2304-974x-2019-8-2-12

Pohorilyi T. (2023), Modeling of non-stationary processes heat and mass transfer according to the cellular model of sucrose mass crystallization, *Ukrainian Food Journal*, 12(1), pp. 80–113, https://doi.org/10.24263/2304-974x-2023-12-1-8

Prada C.D., Cristea S., Mazaeda R. (2015), Hierarchical optimal operation of continuous-batch processes, *IFAC-PapersOnLine*, 48, pp. 294–301, https://doi.org/10.1016/j.ifacol.2015.11.298

Santos R.A., Normey-Rico J.E., Gómez A.M., Arconada L.F., Moraga C.D. (2008), Distributed continuous process simulation: An industrial case study, *Computers & Chemical Engineering*, 32, pp. 1195–1205, https://doi.org/10.1016/j.compchemeng.2007.04.022

Schlumbach K., Pautov A., Flöter E. (2017), Crystallization and analysis of beet and cane sugar blends, *Journal of Food Engineering*, 196, pp. 159–169, https://doi.org/10.1016/j.jfoodeng.2016.10.026

Sidletskyi V. (2019), Steam boiler control system using tensor analysis methods, *International Journal of Computing*, 18(2), pp. 147–154, https://doi.org/10.47839/ijc.18.2.1413

Sidletskyi V., Elperin I., (2019), Integrated control system of the thermal power complex using the tensor analysis methods, *Naukovyi Visnyk Natsionalnoho Hirnychoho Universytetu*, 5, pp. 137–142, https://doi.org/10.29202/nvngu/2019-5/20

Sidletskyi V., Korobiichuk I., Ladaniuk A., Elperin I., Rzeplińska-Rykała K. (2020), Development of the structure of an automated control system using tensor techniques for a diffusion station, *Advances in Intelligent Systems and Computing*, 920, pp. 175–185, https://doi.org/10.1007/978-3-030-13273-6_18

Simoglou A., Georgieva P., Martin E.B., Morris A.J., Azevedo S.F. (2005), A time varying state space approach for sugar crystallization process modelling and monitoring, *IFAC Proceedings*, 38, pp. 27–32, https://doi.org/10.3182/20050703-6-CZ-1902.01580

Singh O. (2019), Exergy analysis of a grid-connected bagasse-based cogeneration plant of sugar factory and exhaust heat utilization for running a cold storage, *Renewable Energy*, 143, pp. 149–163, https://doi.org/10.1016/j.renene.2019.05.012

Sperling S., Hoefnagels J.P., van den Broek K., & Geers M. (2023), A continuum particle model for micro-scratch simulations of crystalline silicon, *Journal of the Mechanics and Physics of Solids*, 182, 105469 https://doi.org/10.1016/j.jmps.2023.105469

Suárez L.A., Georgieva P., Azevedo S.F. (2011), Nonlinear MPC for fed-batch multiple stages sugar crystallization, *Chemical Engineering Research and Design*, 89, pp. 753–767, https://doi.org/10.1016/j.cherd.2010.10.010

Tabassum T., Lim S., Khalghani M.R. (2024), Artificial intelligence-based detection and mitigation of cyber disruptions in microgrid control, *Electric Power Systems Research*, 226, 109925, https://doi.org/10.1016/j.epsr.2023.109925

Tuttle J.F., Blackburn L.D., Andersson K., Powell K.M. (2021), A systematic comparison of machine learning methods for modeling of dynamic processes applied to combustion emission rate modeling, *Applied Energy*, 292, 116886, https://doi.org/10.1016/j.apenergy.2021.116886

Villani E., Pascal J., Miyagi P.E., Valette R. (2004), Object oriented approach for cane sugar production: modelling and analysis, *Control Engineering Practice*, 12, pp. 1279–1289, https://doi.org/10.1016/j.conengprac.2004.04.011

Wang J., Peng X., Huang Z., Zhou H., (2020), A temperature-dependent 3D anisotropic visco-hyperelastic constitutive model for jute woven fabric reinforced poly (butylene succinate) biocomposite in thermoforming, *Composites Part B-engineering*, 208, 108584, https://doi.org/10.1016/j.compositesb.2020.108584

Wilson D.I., Lee P.L., White E.T., Newell R.B. (1991), Advanced control of a sugar crystallizer, *Journal of Process Control*, 1, pp. 197–206, https://doi.org/10.1016/0959-1524(91)85009-8

Zamarreño J.M., Vega P.I., Garcia L., Francisco M. (2000), State-space neural network for modelling, prediction and control, *Control Engineering Practice*, 8, pp. 1063–1075, https://doi.org/10.1016/S0967-0661(00)00045-9

Zhang J., Meng Y., Wu J., Qin J., Wang H., Yao T., Yu S. (2020), Monitoring sugar crystallization with deep neural networks, *Journal of Food Engineering*, 280, 109965, https://doi.org/10.1016/j.jfoodeng.2020.109965

Cite:

UFJ Style

Sidletskyi V., Kukhar O. (2024), Change of crystallization process attributes in a vacuum pan of automation systems, *Ukrainian Food Journal*, 13(2), pp. 366–384, https://doi.org/10.24263/2304-974X-2024-13-2-12

APA Style

Sidletskyi, V., & Kukhar, O. (2024). Change of crystallization process attributes in a vacuum pan of automation systems, *Ukrainian Food Journal, 13*(2), 366–384. https://doi.org/10.24263/2304-974X-2024-13-2-12